Biochemistry

 Volume 42, Number 34 September 2, 2003

Current Topics

Bacterial Ion Channels†

Ian R. Booth,* Michelle D. Edwards, and Samantha Miller

Department of Molecular and Cell Biology, Institute of Medical Sciences, Foresterhill, Aberdeen AB25 2ZD, U.K.

Received June 3, 2003; Revised Manuscript Received July 2, 2003

This is one of the most exciting periods in membrane biology. The last five years has seen the elucidation of the structures of several bacterial ion channels (*1*−*6*). These structures have allowed central questions about the mechanism(s) of selectivity and gating of ion channels to be addressed and have also provided a fertile ground for speculation and model building. What has been particularly significant in this period has been the diversity of structures that has allowed different issues in ion channel function to be discussed in a new light. This review seeks to explore the advances gained from the discovery of bacterial channels but, particularly, from the analysis of their structures.

Ion channels exhibit two major properties, ionic selectivity and gating. The functions of ion channels require fast switch-on rates and transient open states in the millisecond range. The fast transition from closed to open is achieved by gating by specific chemical, physical, and electrical signals. Ion movement through channels takes place at rates approaching those of free diffusion (i.e., $\sim 10^7$ ions/s). This is inconsistent with the presence of strong binding sites that, while offering the potential of discrimination, would slow the turnover to a few events per second. Bacterial channels exhibit gating phenomena on the millisecond time scale similar to those of the higher eukaryotes, responding to chemicals, to changes in membrane potential, and to pressure (*7*−*9*). Bacterial genome sequencing has revealed a variety of homologues of mammalian ion-specific channels (Figure 1). Homologues of a range of K^+-specific channels, Na^+ channels, and Cl^- channels have been identified. Arising from these resources, we now have several crystal structures of bacterial K^+ channels and a structure for the ClC-type chloride channel. Bacterial mechanosensitive channels (*7*), MscL and MscS, whose structures have also been solved (*2*, *10*) form nonspecific channels and will not be considered here.

Structural Motifs in Ion-Specific (K^+, Na^+, Cl^-) Channels. Crystal structures of the bacterial K^+ and Cl^- channels have supplied major insights into the mechanisms of selectivity (*1*, *3*, *11*). The structure of ion binding sites in proteins finds many different solutions in nature, which provide different affinities and specificities. Ion channels exhibit a very high degree of ionic specificity, for example, discrimination between K^+ and Na^+ in P-loop K^+ channels can be of the order of 10^3-fold. The structures of the bacterial channels show that similar solutions have evolved to create the pores in K^+ and Cl^- channels that exhibit both high selectivity and low affinity. In each case the backbone carbonyl (K^+ channels) and amide (ClC) groups create relatively weak binding sites (Figure 2b,c), consistent with rapid ion movement through the channel (*1*, *11*). Amino acid side chains also contribute oxygen atoms to these binding sites, but acidic and basic amino acids are generally avoided to prevent the formation of tight ionic bonds that would hinder the free flow of ions. The specificity is created through the spacing of the carboxyl and amide groups such that they can replace the water molecules that would normally surround the K^+ and Cl^- ions, respectively. In both channels short helices have their dipoles oriented such that an ion of the appropriate charge is "guided" toward the center of the pore (*1*, *3*) (Figure 2a). In addition, the entryways to the channels are enriched for anionic (KcsA) and cationic (ClC) residues so that the substrate ion will be concentrated in the vicinity of the pore.

† The authors' research is supported by The Wellcome Trust (040147) and the BBSRC.

* Corresponding author. E-mail: gen118@abdn.ac.uk. Phone: 44-1224-555852. Fax: 44-1224-555844.

10.1021/bi034953w CCC: $25.00
Published on Web 08/08/2003

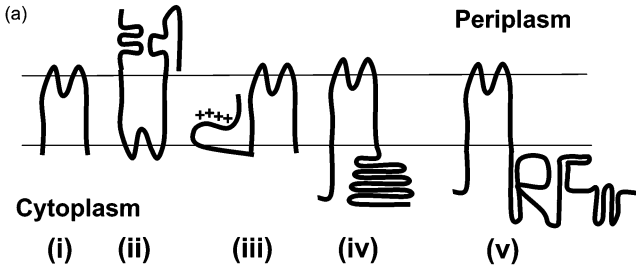

(b)

Ion	Type	Example
K^+	Basic	KcsA
	Voltage-gated	KvAP
	Inward rectifier	KirBac1.1
	Ligand-gated	MthK, GluR0, Kch
	Other	
Na^+	Voltage-gated	NaChBac
Cl^-	Voltage-gated	ClCA, ClCB
	Bestrophin-related	YneE
Other	Glutathione-gated K^+ efflux	KefC
	K^+ uptake proteins	KtrB, KdpA

FIGURE 1: Ion channels in bacterial cells. (a) The figure illustrates the basic structures of the different classes of K^+ channels in bacterial cells: (i) the basic configuration of KcsA; (ii) GluR0; (iii) voltage-gated K^+ channel (note that S1 and S2 have been omitted, and only the voltage sensor, S3a/3b/S4, is shown attached to the basic KcsA core structure); (iv) KirBac1.1; (v) MthK, where the carboxy terminus is the RCK (*4*) or Ktn domain (*55*) carrying the Rossmann fold. (b) Bacterial ion channels. The K^+ channels were subclassified on the basis of BLAST searches using the KcsA, MthK, KirBac1.1, and KvAP protein sequences. Several homologues were observed for each class. However, there are many K^+ channel homologues related to KcsA that possess additional amino-terminal or carboxy-terminal domains that are not similar to the four crystallized examples. These sequences have been noted as "other".

Despite the similar strategies for pore construction the structures of the K^+ and Cl^- channels could not otherwise be more different (Figure 2a,b). The K^+ channel pore arises from the junction of the four identical subunits and is asymmetrically arranged within the plane of the membrane, closer to the periplasmic surface than the cytoplasm. In contrast, ClC channels are dimeric, but each ClC chloride channel subunit has an independent pore created from several short helices that only penetrate partway across the membrane (*12*, *13*). Chloride channels have arisen from an ancestral duplication, and in these two aspects they resemble the construction of the aquaporin (*14*), although ClC is a much more complex and larger protein.

(A) Potassium Channels. The structure of the K^+ channel was first defined by the resolution of the crystal structure of the 160 amino acid *Streptomyces lividans* KcsA channel (*15*) to 3.2 Å (*1*). The simplest K^+ channel subunit consists of two transmembrane spans, TM1 and TM2, separated by a short pore helix and the P loop that together define cation specificity (Figure 1a, i). Remarkably, there are very few examples of K^+ channel proteins as small as KcsA in the bacterial genome database; most possess either amino-terminal or carboxy-terminal extensions. Three further structures of K^+-specific channels, which represent the wider group of bacterial K^+ channel proteins, have essentially confirmed the KcsA pore architecture and have given insights

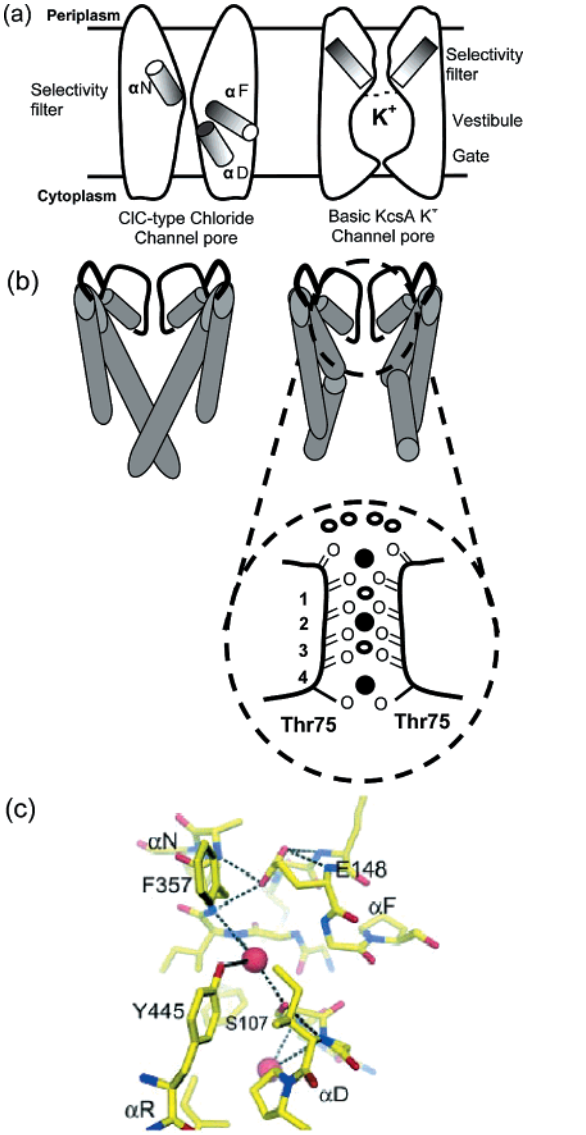

FIGURE 2: Ion-selective pores for K^+ and Cl^-. (a) Dipole arrangements in the ClC channel and K^+ channel. In ClC the positive end of the dipole (dark shading) is oriented toward the center of the membrane and "focuses" the Cl^- ion at the neck of the selectivity filter. In the K^+ channel the inverse arrangement is observed with the positive end of the dipole oriented to the membrane surface positioning the negative dipole toward the vestibule end of the selectivity filter. Note also that the filters are positioned centrally within the membrane for the Cl^- channel but close to the periplasmic surface in the K^+ channel. The filters are each approximately 12 Å in length. Cartoon after MacKinnon (*3*). (b) This panel illustrates two of the four subunits that make up the symmetrical tetramer of the closed state of KcsA. In the left-hand panel the TM2 helices form the lining of the channel, and their interaction at the cytoplasmic face forms the gate of the channel. The right-hand panel illustrates the open conformation of the channel, as found in the MthK open channel structure (*41*), with an expansion of the pore selectivity filter region with K^+ ions (filled circles) in positions 2 and 4 and with a K^+ ion at the outer neck of the filter. Water molecules (open circles) surround the K^+ outside the filter but are replaced by carbonyls or oxygen atoms of Thr75 in positions 2 and 4, respectively. Positions 1 and 3 are occupied by water molecules. Figures inspired by refs *21* and *41*. (c) The molecular detail of the chloride channel (*3*) selectivity pore (reproduced with permission from ref *11*. Copyright 2003 American Association for the Advancement of Science). The red sphere represents the chloride ion interacting with Y445, S107, and backbone amides of the αN helix. Note that the gating residue E148 interacts in a similar way to the chloride ion with amide bonds of the αN and αF helices.

into the structure and role of the adjacent domains (*5*, *6*, *16*). The TM2 helices line the pore, and the TM1 helices interact with lipid. The TM2 helices cross the membrane at an angle of 25° to the axis of the pore and are slightly kinked at the periplasmic ends so that they splay outward (Figure 2b). Short pore helices have the negative ends of their dipoles pointing toward the center of the vestibule below the selectivity filter. Here the focused dipoles help to stabilize the K^+ ion located in the vestibule. The recent structure of KirBac1.1, which has been crystallized with its amino and carboxy termini relatively intact, has the pore helices misaligned such that the dipoles do not contribute as strongly to ion binding in the vestibule as in KcsA (*16*). It has been suggested that this collapses the vestibule into a closed state.

In the KcsA crystal structure, TM2 helices cross close to the cytoplasmic face (Ala111 in KcsA; Phe146 in KirBac1.1), effectively sealing the K^+ conducting path across the membrane (*1*, *16*). In the crystal structure of KcsA a single K^+ ion surrounded by structured water is visible in the vestibule whereas in KirBac1.1 only diffuse electron density is seen in this region (*17*). It has been suggested that the vestibule K^+ ion in KcsA is held in place by weak hydrogen bonds via less structured water to the side chains of Thr107 and backbone carbonyls of TM1. This places a hydrated K^+ ion in line with the selectivity filter, and with the channel closed, there is effectively 2 M K^+ in the vestibule (*17*). Since dehydration reactions are very rapid relative to the rate of passage of the ion, the hydrated state of this ion is no barrier to ion conduction.

The selectivity filter, or pore, of K^+ channels has the consensus sequence $T_{75}VGYG_{79}$ (using the KcsA numbering) (*18*−*20*). The peptide backbone of this sequence is oriented such that four rings of carbonyls project into the lumen of the pore and the valine and tyrosine side chains are oriented away from the pore (*1*, *21*). These side chains make specific contacts with tryptophan residues in the pore helix, forming a sheet of aromatic residues that holds the peptide backbone in position. Cation selectivity is significantly determined by these interactions since they control the diameter of the pore. Four stacked binding sites (1−4, Figure 2b), each of which can be occupied by a single ion, are created by the backbone carbonyl groups of residues Thr75, Val76, Gly77, and Tyr78 and by the side-chain oxygen of Thr75 located below, at the entrance to the vestibule. Above the selectivity filter the backbone carbonyl of Gly79 contributes to a binding site, probably promoting ion dehydration by providing four of the eight oxygen atoms needed to satisfy the K^+ ion (*21*). Analysis of the kinetics of K^+ and Rb^+ movement has been correlated with crystal structures solved in the presence of each of these ions at both low and high concentrations. These studies suggested that electrostatic repulsion between K^+ ions ensures that alternate binding sites are occupied by ions with the intervening site occupied by a water molecule (*21*). For example, ions may be bound at either sites 1 and 3 or sites 2 and 4 (Figure 2b). If sites 1 and 3 are occupied, the entry of another K^+ ion to a vacant outer position would push the ion in site 1 to site 2 and that in site 3 to site 4 simply by repulsion. The exit of the ion from site 4 into the vestibule would complete ion translocation from out to in. Such a simple mechanism explains why ion translocation through the channel approaches the rate observed for free diffusion and why ion channels are freely reversible.

(B) Inward Rectifier Channels. New structures show how the basic architecture of K^+ channels can be modified to allow for essentially unidirectional ion movement in the inward rectifier (KIR) class of K^+ channels (*16*, *22*) (Figure 1a, iv). KIR channels have the basic KcsA channel structure flanked by conserved amino- and carboxy-terminal domains. By making fusions of different lengths of the two flanking domains of mGIRK (mouse), the structure of the cytoplasmic pore, which lies immediately below the vestibule and seal of the channel, was solved. Tetrameric assemblies were observed that contained a central 7−15 Å pore that extends 30 Å below the plane of the membrane and that was predicted to be colinear with the pore of the channel. This structure (*22*) has been elegantly supported by determination of the structure to 3.65 Å of the bacterial KIR channel KirBac1.1 (*16*) (Figure 3). The N-terminal domain forms an integral part of the cytoplasmic pore domain through a short β sheet that interacts with the carboxy-terminal domains of the adjacent subunit (*16*, *22*). This interaction places constraints on the transmembrane helices to which these domains are attached, which may aid the transmission of the gating signal. Flexible linkers connect the cytoplasmic domain to the channel, but it is believed that the "portal" created between the linkers is unable to allow K^+ ions to exit from the channel protein due to ionic repulsion by basic residues at this location (*16*). The K^+ ion is expected to traverse a distance of ∼88 Å, rather than the maximum of ∼12 Å in KcsA or MthK, before reaching the bulk phase. Consequently, the K^+ must pass through the cytoplasmic pore that is subject to blocking by Mg^{2+} or polyamines (*23*−*25*). Glutamate residues (Glu187 and Glu258) that project into the lumen of the cytoplasmic pore have been implicated in the binding of Mg^{2+} and polyamines (*16*) (Figure 3a). Polyamine binding is predicted to be favored in the bacterial channel by the spacing of the two rings of negative charge.

(C) Voltage-Dependent K^+ Channels. Voltage-gated K^+ channels share the basic organization of the K^+ pore described above but, in addition, have amino-terminal membrane segments, one of which, S4, carries several basic residues separated by hydrophobic amino acids $(R/Kxx)_{5-6}$ (*26*−*28*). This structural feature is responsible for voltage dependence of the channel. It has long been held that movement of these residues in response to changes in the membrane potential is responsible for pore opening (*28*). Gating requires the equivalent of 12−14 electron charges moving through the whole membrane field. Given the tetrameric nature of the channel, this meant that 3−3.5 charges per subunit had to be relocated across the membrane (*28*). How could this be achieved? Jiang and colleagues have proposed a solution based on the crystal structure of KvAP from *Aeropyrum pernix*, a bacterial homologue of voltage-dependent K^+ channels (*6*, *29*) (Figure 1a, iii). The structure of KvAP, complexed with an Fab fragment, was resolved to 3.4 Å. The crystallization conditions appear to have trapped the open configuration of the channel (*29*). The selectivity filter and overall structure of the K^+ pore share strong similarities with KcsA, whereas the alignment of the TM2 helices (S6 in KvAP) bears a stronger resemblance to the MthK channel. The voltage sensor, which is directly attached to the outer helix (S5), might exert its influence on channel opening by pulling on S5 to allow bending at the residue in S6 equivalent to Gly83 in KcsA. In the crystal

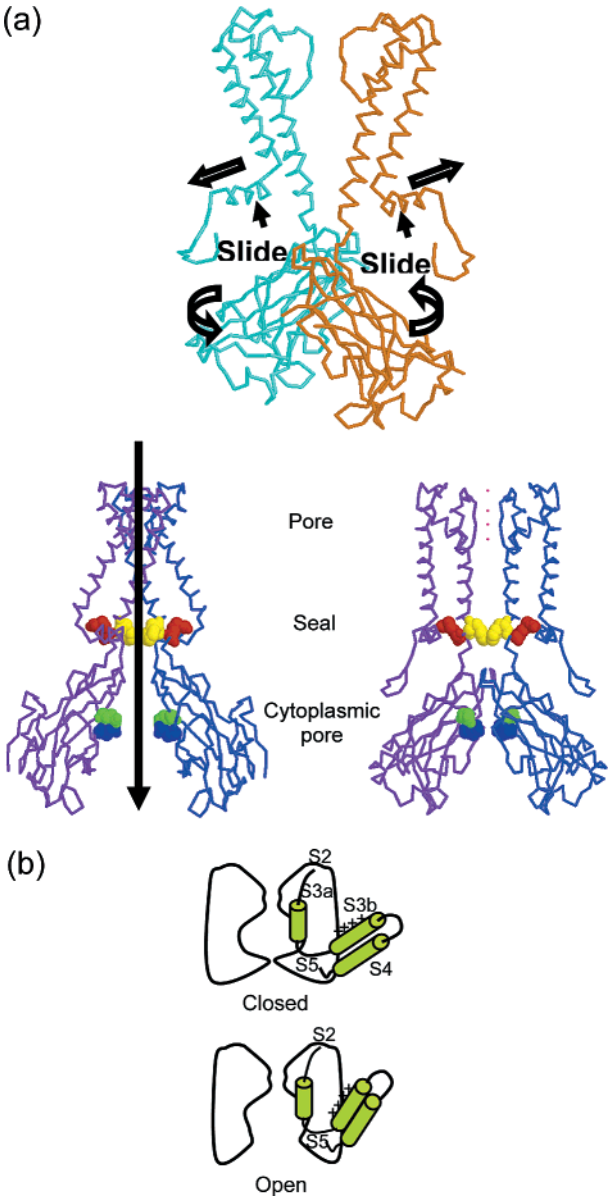

FIGURE 3: Voltage-gated and inward rectifier channels. (a) Overview of the KirBac1.1 structure (*16*). Upper panel: Two subunits of Kirbac1.1 have been removed for clarity to display the position of the slide helix relative to TM1. (created with the Kirbac1.1 PDB file with the permission of the authors). The twisting movement (curved arrow) of the carboxy-terminal domains is thought to exert a pull (horizontal arrow) on the slide helix leading to bending and rotation of TM2 and consequent opening of the pore. Lower panel: Two different views to show the positions of R418 (red), F146 (yellow), E187 (blue), and E258 (green). A black arrow indicates the path that the K^+ ion would take through the open channel. The figures were created using Chime. Note the interaction of the amino-terminal β sheet with the carboxy-terminal domain. (b) Schematic of the voltage sensor paddle attached to the core S5−S6 P-loop unit. The voltage sensor S3a−S3b/S4 is shown in green in the proposed closed (membrane potential negative inside) and open (membrane depolarized) channels. Although the S1 and S2 segments have been omitted, the connection between S3a and S2 is shown on the basis that S1 and S2 will form relatively conventional transmembrane helices; note, however, that this would require the S1 helix to adopt an N-terminal out configuration. In response to the membrane potential (negative inside) the sensor paddle is expected to be drawn toward the cytoplasmic surface of the membrane. On depolarization the sensor moves outward, pulling on S5, allowing S6 to bend and the channel to open. It is worth noting the strong similarity between this model and that proposed for MscS sensing of membrane voltage (*10*).

structure the first two transmembrane helices (S1 and S2) form a concentric ring around the S5/S6 pores, with S3 and S4 lying outside that ring (*6*). The structure leads to the proposition of a significant variation from the conventional depiction of S1−S4 as four α helices. In particular, it is proposed that S3 and S4 are actually three helices, S3a, S3b, and S4, with the latter pair forming an antiparallel helix−turn−helix, "the voltage-sensor paddle" (Figure 3b). The voltage-sensitive arginine residues are located in S3b, which connects to S3a via the S3 loop (*6*). In the crystal structure S3a lies coaxial with the pore axis, and the paddle is parallel to the cytoplasmic face of the membrane. A sharp turn ends S4 and leads into S5, the outer helix of the pore, and readily explains how movement of the paddle could lead to displacement of this helix, allowing bending of S6 and channel opening. Overall, the voltage sensor is seen as being a highly flexible protein domain that interacts loosely within the membrane phase with the pore-forming S5/S6 domain. Flexibility was demonstrated by the separate crystallization of the S1−S4 domain, which exhibited similar organization of its core S3a−S3b/S4 elements to that seen in the whole channel protein (*6*). The essential separateness of the voltage sensor and the pore is supported by the ability of the S1−S4 domain to be grafted onto KcsA pore domains to form a fully functional channel (*30*).

Studies with antibodies specific for the paddle and with toxins have supported a model in which the voltage sensor is accessible from different sides of the membrane in response to membrane depolarization (*28*, *29*). Antibodies applied at the periplasmic face of the channel caused progressive inhibition dependent upon cycles of membrane depolarization. No inhibition was evident until the membrane had been depolarized. Tarantula venom, which binds at the S3/S4 sequences, inhibited from the periplasmic face, and the rate was enhanced by cycles of depolarization. Further support for the model came from accessibility of biotinylated single cysteine residues to avidin applied from different sides of the membrane. Residues on the upper face of the paddle (e.g., G112C) were accessible from the external face, whereas those on the lower face (e.g., I127C) were accessible from the internal side. Two cysteine mutants (L122C and L121C) exhibited inhibition by avidin when applied from either the external or internal face. This was interpreted as evidence that the paddle can translocate the biotin label from one surface to the other in response to depolarization in the manner suggested for colicin translocation (*31*). The data support the model that the S3a−S3b/S4 paddle is mobile within the membrane and affords a mechanism for gating the channel in response to membrane depolarization.

(D) GluR0 Channels. A bacterial homologue of the GluR2 AMPA[1] channel has been identified in *Synechocystis* (*32*). The GluR0 protein exhibits an inverted KcsA-like core structure (selectivity filter located close to the cytoplasmic face of the membrane) and flanking periplasmic amino- and carboxy-terminal domains (Figure 1a, ii). Strong conservation of residues known to be critical for glutamate binding and for structure was observed in the periplasmic S1 and S2 domains (*32*). Purified S1−S2 domains of GluR0 bound L-glutamate with relatively high affinity, but the amino acid

[1] Abbreviation: AMPA, (*S*)-amino-3-(3-hydroxy-5-methyl-4-isoxazole).

could not be displaced by the classical GluR agonists (e.g., AMPA). A range of physiological amino acids were found to antagonize L-glutamate binding. Using a protein fusion between rat GluR and GluR0 to obtain expression in oocytes, currents were observed when either glutamate or other amino acids that bound strongly to the S1/S2 domain were added. Unlike the eukaryotic channels, which are relatively nonspecific, GluR0 was K^+-specific (*32*). However, accumulation of Na^+ on the extracellular side of the pore was observed to block K^+ conduction. The recent crystallization of the GluR0 S1/S2 domains, and their biophysical characterization, has further reinforced the homology between this channel protein and its eukaryotic counterparts (*33*, *34*). The domains form a bilobate structure that in the eukaryotic protein undergoes a major conformational change upon ligand binding (*33*−*35*). Thus conservation of sequence is likely to be matched by strong mechanistic similarities.

(E) Na^+ Channels. Bacterial Na^+ channels lag behind the K^+ and Cl^- proteins in terms of the sophistication of their analysis, due to their relatively recent discovery. The genome sequence for the alkalophilic halophile *Bacillus halodurans* led to the discovery of a protein that strongly resembled the domains of mammalian Na^+ and Ca^{2+} channels (*36*). The database of bacterial genome sequences contains a small number of proteins (about six) that are similar in length to NaChBac and which possess both the voltage sensor and the more typical P-loop sequence TLESW (underlined text indicates strongest conservation). Other related proteins are only weak candidates for Na^+ channels due to degeneration of the P-loop sequence or loss of amino-terminal sequences. Most of these proteins retain perfect voltage sensor sequences. The current through the NaChBac channel is carried by Na^+ with a weak permeability to Ca^{2+} but no significant conduction of K^+ or Cs^+ (*36*). NaChBac is expected to be a homotetramer on the basis of its similarity to KvAP. In higher organisms the voltage-gated Na^+ channel protein contains four "repeat" domains, each of which has the structure akin to the KvAP channel discussed above, and it is not unreasonable to expect that the structure of the latter can be used to make models of the bacterial Na^+ channel.

(F) Chloride Channels. In the dimeric ClC Cl^- channel the pores created by each monomer are well separated, and the protein surface between is strongly electronegative, which is consistent with the known independent operation of the pores (*37*, *38*). The protein contains 18 α helices, which vary significantly in their length and membrane crossing angles (*3*). Unlike the K^+ channel, the selectivity filter is positioned midway across the membrane and is created by several short helices (αN, αF, and αD) that have their amino termini directed toward the eye of the selectivity filter. The positive end of the dipole is oriented toward the pore, a structure that ensures the Cl^- ions will be funneled into the filter (Figure 2a). Peptide bond amides from αN are available to bind the ion, augmented by the side-chain oxygen atoms of Ser107 (αD) and Tyr445 (αR) (Figure 2c). On either side of the pore are water-filled vestibules that carry a number of basic residues that might be expected to concentrate the Cl^- ions at the entrance to the channel. In contrast to the K^+ channel, the Cl^- channel essentially has only room for a single ion in the pore, although the recent crystal structures show how three ions can be accommodated in a single channel (*11*). In this structure one of the additional ions lies below the selectivity filter coordinated to main-chain amide groups from the amino-terminal end of helix αD and also forms bonds with water molecules in the vestibule. The third ion is only seen in mutant forms of the channel in which Glu148 is replaced by Ala or Gln, when the ion replaces the gating glutamate residue directly between the amino termini of the αN and αF helices (i.e., just above the selectivity filter) (Figure 2c). An activator site is known to be present on eukaryotic ClC channels and displays a significantly different halide preference to the channel itself (*39*). Little is known about this site in the bacterial channels (*40*).

Opening the Channel. The open channel can be seen to arise from two linked but essentially separate changes in the structure of the channel protein. The ion-conducting pathway has to be opened to connect the bulk phases on either side of the selectivity filter, and a signal has to be perceived. Although the latter will precede the former, it is easier to discuss signal perception once one has dealt with the opening of the ion-conducting pathway.

(A) Structural Changes Involved in Opening the Ion-Conducting Pathway. Solution of the structure of the MthK channel in the open state suggested that TM2 pivots about a conserved glycine residue (Gly83 in MthK), such that the vestibule becomes continuous with the bulk phase (*5*, *41*). Supporting data for this model come from the KirBac1.1 channel structure, although the critical hinge residue is probably not at the position equivalent to Gly83 (see below) (*16*). The TM2 helix, which is almost straight in the vestibule region of KcsA, bends almost 30° in the MthK structure. Gly83 is highly conserved among members of this family, and analysis of helix movements during opening of KcsA, using site-directed spin labeling, is consistent with the bending of this helix. EPR analysis of site-directed spin labels has the advantage of relatively "real time" analysis of protein movement. Data obtained by this route are consistent with the view of the open channel developed from the MthK crystal structure (*42*). Thus, it was observed that the upper reaches of the vestibule and the selectivity filter were relatively immobile during gating of KcsA by acid pH but that large changes in position were observed for residues at the cytoplasmic end of TM2, the channel-forming helix. Much smaller movements were observed in TM1. The prediction was that TM2 would swing away from the axis of symmetry of the channel (*42*) (Figure 2b), as was subsequently observed in the structures of MthK and KirBac1.1. In such a model, once this closed to open transition is made, the movement of ions is only constrained by the time required to pass through the filter. Previous data on the inhibition of K^+ channels by large organic cations applied from the cytoplasmic side of the membrane and models of inactivation by amino-terminal "balls" are given greater coherence by the MthK structure (*41*, *43*, *44*).

Much less is known about the gating of ClC channels at the molecular level, but analysis of mutant ClC proteins has led to a strong model (*11*). The *Torpedo* ClC-0 channel is considered to be homotropically activated by Cl^- ions and is voltage gated (*39*, *45*). To what extent these properties are shared by the bacterial channels is not yet known, but the crystal structure provided a powerful analytical tool for understanding gating (*11*). The Glu148 residue described above is moderately conserved and is positioned above the pore such that the γ-carboxylate group provides electrostatic

repulsion, possibly as a pseudosubstrate. The recent crystal structure makes it explicit that relocation of this residue is essential to allow free diffusion of chloride ions through the channel pore. Combining crystallographic analysis of *Escherichia coli* ClC mutants with electrophysiological analysis of equivalent mutations in the *Torpedo* ClC-0 channel expressed in oocytes, MacKinnon and colleagues have provided strong data in support of the role of Glu148 in gating (*11*). Mutation of Glu148 to Ala, Gln, or Val creates an open channel. ClC-0 channels exhibit voltage-dependent gating: the gate closes at negative (inside) membrane voltage and opens when the channel is depolarized. Closure of the gate, on imposition of a membrane voltage (negative inside), lowers the whole cell current in oocytes expressing ClC-0. In E166A, E166V, or E166Q (Glu148 in *E. coli* ClC) the current is maintained constant throughout voltage changes. The current−voltage relationship of E166Q can be mimicked in the wild-type protein by acidification to pH 5, which suggests that the mutational change is equivalent to protonation of the Glu166. Physiological analysis of the role of ClC in *E. coli* has shown that the channel is activated by acid pH in a manner that is equivalent to the change seen at pH 5 in ClC-0 (*46*). Crystal structures of the *E. coli* ClC mutants E148A and E148Q were consistent with this view of the gating. Minimization of the side chain in E148A led to an extra chloride ion in the monomer, positioned equivalent to Glu148, creating a queue of chloride ions through the channel (*11*). In the E148Q mutant the glutamine was observed to be relocated into the extracellular vestibule, thus opening the channel pathway. MacKinnon has pointed out that the small movement required for Glu148 to block or open the pathway means that the conformational change in one monomer can be independent of the other subunit of the dimer, leading to separate rather than coordinated opening and closing.

(B) Gating: Transmission of the Gating Signal. The first major event in the opening of the channel is the transmission of the gating signal, about which comparatively little is known for the bacterial K^+ channels but rather more for Cl^-. The ClC Cl^- channel of *E. coli* has been shown to have a role in protection of cells against extremely acidic conditions. When cells are exposed to low pH (pH ~3), they require the activity of acid tolerance systems for long-term survival (*46*). One of these systems is based on conversion of externally supplied glutamate to γ-aminobutyrate in the cytoplasm and their exchange via an antiport (*47*). In some way the ClC channel is required for the optimum activity of the glutamate-based acid protection system. Correspondingly, *E. coli* ClC was observed to be gated by acid pH (*46*).

The KcsA channel is also activated by low pH (*48*), and this has been demonstrated to be physiologically significant by expression of the wild type and tryptophan-scanning mutants in *E. coli* (*49*). Observation of Ca^{2+} ions bound in MthK RCK (Ktn) domains led to the proposal that this is a Ca^{2+}-gated channel (*5*). Electrophysiological analysis also showed that the channel could be gated by Ca^{2+}, but the affinity for Ca^{2+} was in the millimolar range, which exceeds physiological concentrations in bacteria by up to 10^3-fold. Consequently, the actual significance of the bound Ca^{2+} is in doubt, especially as it is not uncommon for protein crystals to bind ions that aid structure formation.

The only K^+ channel for which the physiological gate is truly established is KefC, and doubt has been cast on whether it is a channel or transporter. The original basis for suggesting that it is a channel was that the rate of K^+ translocation approached that of channels (i.e., 10^6-10^7 ions/s) and that the amino acid sequence of the protein exhibited channel-like features (*50*). What is not in doubt is the physiological role of KefC and its gating mechanism (*50*−*53*). The channel is maintained closed by the binding of glutathione, and related peptides, and is activated by glutathione adducts. Adducts are formed by reaction between electrophiles and glutathione and are intermediates in the detoxification of these toxic compounds (*54*). The consequence of channel activation is rapid K^+ loss that leads to acidification of the cytoplasm that in turn protects the cell against damage that the electrophile would otherwise cause.

The large-scale protein movements made by TM2 during the opening of K^+-specific channels make them suitable to gating by changes in structure of more distant parts of the protein. MthK has RCK domains attached to the carboxy terminus of TM2, which potentiate gating as a result of conformational changes in this domain. The RCK and Ktn domains are built on the scaffold of the Rossmann fold and have been observed as a structural element of K^+ channels and transporters from bacteria to man (*4*, *55*). In RCK domains the nucleotide binding pocket is less stringently conserved than in Ktn (*55*). Mutational analysis has identified roles for the RCK/Ktn domain in gating BK channels in man, Kch in *E. coli* (C. Kung, personal communication), and the KefC K^+ efflux system in *E. coli* (*56*, *57*). A number of mutations that modify the gating of the KefC channel, leading to a high rate of K^+ leakage, have been mapped to the Ktn domain, and others lie in the HALESDIE loop in the membrane domain (*56*). The latter most probably directly affect the pore, whereas those in the Ktn domain affect gating. Genetic data have pointed to the importance of salt bridges between the Ktn domain and a membrane loop (HALESDIE) in gating the channel (*55*). In particular, it was demonstrated that charge reversal at a conserved Ktn residue, R527, could be compensated by the opposite charge change within the HALESDIE loop. This salt bridge may be required to retain the correct juxtaposition of sequences. Precisely how changes in glutathione structure gate the channel remains unknown.

RCK/Ktn domains are capable of forming higher order oligomers: that proposed for MthK is an octomer created by translation initiation from two sites within the *mthK* mRNA such that, in addition to full-length channel protein, separate domains are made, allowing the tetrameric channel protein to have eight Ktn domains (*5*). A similar secondary translation initiation site has been observed in the Kch channel (C. Kung, personal communication). This is a tetrameric K^+ channel of the same broad type as KvAP (but lacking a strong voltage sensor motif) and has an RCK domain at its carboxy terminus. Recently, mutants that exhibit altered gating of the Kch channel, corresponding to a more frequent open state, have been isolated in the RCK domain (C. Kung, personal communication). The mutations could be suppressed by specific changes that are expected to disrupt the selectivity filter. It was noted that elimination of the translation start site for expression of the separate RCK domain did not suppress the gain of function mutations,

despite the elimination of expression of this extra domain. These data cast doubt on the significance of an octameric assembly, if only for Kch.

There are four crystal structures for RCK/Ktn domains: from the Kch (*4*) and MthK (*5*) channels and from two K^+ transporters of the KtrA and TrkH class (*55*). No ligand was observed with the Kch protein, and Ca^{2+} was observed in the MthK. The transport proteins had either NAD or NADH bound and were observed to form tetramers in the presence of the ligand (*55*). There is a complex scaffold of interactions possible between Ktn domains depending on whether they form dimers, tetramers, or octamers. In the simple dimer the α6 helices of each subunit cross over and make contacts with the edge of the Rossmann fold domain of the other subunit. This is the "flexible" interaction (*5*, *55*). Other than this crossover there is no substantial protein−protein contact, and the hinge, formed where the two α6 helices cross over, forms a zone of flexibility that allows different angles in the individual structures. When the tetramer forms, the dimers are held together by hydrophobic interactions (known as the "fixed" interface). The lack of specificity in these interactions means again that the crossing angles are different in each channel. Alternating fixed and flexible contacts between subunits create the octameric MthK structure. In the MthK octamer model, a subunit that is covalently attached to TM2 alternates with one that has been synthesized from the secondary translation site. The upper surfaces of the Ktn domains, which bear the groove of the Rossmann fold that could be occupied by NAD(H), line a pore that is colinear with that of the channel (*5*). Potassium ions entering the channel would have to pass through this structure in a manner similar to that suggested for the KirBac1.1 channel. Most of the Ktn domain proteins have extra carboxy-terminal domains, the sequence of which more or less defines the subfamily of proteins to which the Ktn-bearing protein belongs. In MthK these domains lie peripherally to the ring of Ktn domains and are suggested to be a stabilizing element. The unique nature of these sequences and their absence from structures other than MthK make it difficult to determine whether they have the same physical relationship in all structures. Overall, the Ktn domain appears to be utilized differently in each system, and consequently, it would not be surprising if these ancillary domains were also positioned uniquely to achieve specific interactions or functions.

Gating via Ktn domains is not understood. The alternative structures of the two bacterial transporter Ktn domains with different ligands bound offered up a model that variations in the crossover angle of the α6 helices would result in lateral force being applied to TM2 helices, causing them to swivel to the open position (*55*). A similar observation has been made for the RCK domain of Kch and MthK: although the fixed domains are essentially superimposable, the angles created by the flexible domains are quite different (*5*). Although the cytoplasmic domains of KirBac1.1 are quite different in structure and sequence to Ktn domains, a similar pivoting has been proposed to result in opening of the channel (*16*) (Figure 3b). The parallel between the Ktn domains and periplasmic binding proteins has been pointed out. Here, entry of a solute into its binding site, which is positioned at the base of the cleft between the two domains, causes a movement of the domains relative to each other (*58*). The fixed and flexible interfaces allow for cooperativity to be generated between channel subunits. In the tetrameric and octameric assembly, the binding of ligand to one subunit will cause a change in the crossing angle of the α6 helices that is then transmitted to the adjacent pair of subunits. The affinity of the next pair of subunits for the ligand may be influenced by this conformational change, giving rise to cooperativity (*5*).

In KirBac1.1 a significant role for channel gating is suggested for the amino-terminal slide helix that lies parallel to the plane of the membrane (*16*). This helix may be important for stabilization of the closed state and for displacement of the outer (TM1) helices during opening, thus making room for the bending of TM2 as suggested from the structure of MthK. In the closed state, the conserved Arg148 interacts with the negative end of the slide helix, another example of the use of dipoles in channel architecture. Opening is believed to involve the rotational movement of the domains that make up the cytoplasmic pore, leading to displacement of both the blocking Phe146 and Arg148 (Figure 3a). This simultaneously releases the slide helix and allows the outer helices to move away, allowing the hinging on TM2 and the formation of the open pathway for ion conduction. It is suggested that Gly134, which is the equivalent of Gly83 in KcsA, is probably not involved in bending TM2 because it is not completely conserved in this family of channels (*16*). However, the conservation of small residues at this position has been proposed to be important for allowing TM2 to bend after the selectivity filter. Gly143, which is highly conserved in Kir channels, is the hinge position for TM2. Thus, while K^+ channels may use the same basic mechanisms of opening the vestibule to the cytoplasm, each family may have evolved a slightly different hinge position, possibly through co-evolution with the gating domains and their associated linkers.

Roles of Ion Channels in Bacterial Physiology. Different pieces of this particular jigsaw have been assembled, but the whole picture is not available for any organism. While ion channels mediate ion movements across the membrane, each gating event is likely to lead to only minimal changes in the pools of ions in the cytoplasm. A channel open for 1 millisecond and conducting 10^7 ions/s will only move 10^4 ions, and a bacterial cell might contain $\sim 10^8$ K^+ ions, $\sim 10^6$ Na^+ ions, and 10^5 Cl^- ions (assuming ~ 2 μL of cytoplasm/10^9 cells and 300, 1, and 0.1 mM, respectively, for the intracellular concentrations of K^+, Na^+, and Cl^-; Ca^{2+} has been ignored for this analysis but would be expected to be low micromolar). The most dramatic changes arising from gating are in the pools of ions that are traditionally excluded from cells (Cl^- and Na^+), whereas the activity of the K^+ channel might more significantly influence the membrane potential (*59*). A role for the alkaline pH-dependent gating of a Na^+ channel has been proposed on the basis of the need for the rapid entry of Na^+ in response to overalkalinization of the cytoplasm. The Na^+ ions that have entered provide the substrate for the Na^+/H^+ antiports that mediate acidification of the cytoplasm (*59*). A sustained open state (i.e., seconds rather than milliseconds) of the voltage-gated Na^+ channel, of the type seen in *B. halodurans*, would allow bulk movement of Na^+ entry competent to allow cytoplasmic acidification. As pointed out above, it is clear that there are also variants of the NaChBac channel in bacterial genomes that lack obvious voltage sensors that might have roles in

pH homeostasis. At the opposite end of the pH scale, the Cl^- channels ClcA and ClcB (formerly EriC and MriT) have been shown to have a role in protection against acid stress as discussed above and elsewhere (*46*, *60*). However, preliminary data from the authors' laboratory suggest further roles for these ion channels in the normal vegetative growth of *E. coli*.

With the K^+ channels, insights into physiological function have been much harder to find. Mutants lacking KcsA in *S. lividans* and Kch in *E. coli* suffer no discernible disadvantage. This may reflect the limitations of the methods used to look for physiological roles, but clearly the data available suggest no central role for the channels. The most plausible reason for possessing K^+ channels, particularly those with voltage sensors, is the maintenance (or regeneration) of the membrane potential. Intracellular K^+ concentrations are high (~300 mM) in most organisms, and the environment rarely contains more than 10 mM. A substantial K^+ gradient could sustain the membrane potential during long periods of starvation, and this may either enable a basal level of ATP synthesis or sustain the integrity of the cell. Conversely, some K^+ transporters are now being considered to be evolved from ancient K^+ channels (*61*, *62*). In such systems the desired effect would be inward movement of the cation, which would depolarize the membrane. Generating a substantial K^+ gradient would require that the open probability is low relative to the capacity to generate the membrane potential. The ability of mutants of KcsA (*49*) and MscL channels (W. Epstein, personal communication) to generate K^+ pools sufficient to sustain growth at low external K^+ concentrations (~5 mM) in *E. coli* mutants lacking the three major uptake systems is a strong demonstration of this potential among channel proteins.

Ion channels may also play more subtle roles in generating a response to particular chemical signals. The KefB and KefC systems of *E. coli* are the most clear-cut examples (*52*, *63*, *64*). In the presence of electrophiles the cytoplasmic glutathione pool is rapidly converted into a pool of glutathione adducts as the first step in detoxification. The channels are maintained closed by the binding of glutathione and are activated by specific adducts. Activation of the channel by the formation of glutathione adducts leads to bulk K^+ efflux accompanied by acidification of the cytoplasm. Extensive experimentation has shown that this acidification is crucial for cells to survive exposure of the electrophiles that form adducts with glutathione (*54*). More subtle roles might be associated with the inward rectifier family and by the GluR0 family. The perception of intracellular or extracellular signals, respectively, may be used to elicit changes in K^+ permeability, which would modulate the membrane potential during short bursts of activity or could, under sustained firing, change the cytoplasmic pH. The cell might then use these changes as cues for modifications in either metabolism or gene expression. Clearly, for the adventurous spirit there is considerable scope for speculation and investigation.

Conclusions. The last five years has seen an exciting and stimulating time for advocates of bacterial channels. The progress described here has been matched by studies of the other major classes of bacterial transporters (*65*), the porins (*14*, *66*, *67*) and the mechanosensitive channels (*2*, *10*). Genome analysis has identified other homologues of mammalian channel proteins; e.g., *E. coli* possesses a homologue of the human bestrophin chloride channel (*68*, *69*), about which relatively little is known (M. Pallen, personal communication). Others have begun to reconfigure their models for bacterial K^+ uptake proteins to map onto a tetramer of KcsA, with the additional proviso that these would have an asymmetric selectivity filter due to the lack of conservation of the repeat structure of the pore-forming domain (*61*, *62*). What is clear from these studies is that the basis for selectivity and gating in ion channels evolved early in the history of life on earth and has been deployed by bacteria for millions of years for the sophistication of their physiology.

ACKNOWLEDGMENT

The authors thank the following for advice, encouragement, and prepublication manuscripts: Paul Blount, Doug Rees, Randal Bass, Roderick MacKinnon, Senyon Choe, Tarmo Roosild, Mark Pallen, Chris Miller, Eduardo Perozo, Ching Kung, Sergei Sukharev, Evert Bakker, Wolf Epstein, and not least current and past members of the bacterial physiology research group at the University of Aberdeen.

REFERENCES

1. Doyle, D. A., Cabral, J. M., Pfuetzner, R. A., Kuo, A. L., Gulbis, J. M., Cohen, S. L., Chait, B. T., and MacKinnon, R. (1998) *Science 280*, 69−77.
2. Chang, G., Spencer, R. H., Lee, A. T., Barclay, M. T., and Rees, D. C. (1998) *Science 282*, 2220−2226.
3. Dutzler, R., Campbell, E. B., Cadene, M., Chait, B. T., and MacKinnon, R. (2002) *Nature 415*, 287−294.
4. Jiang, Y. X., Pico, A., Cadene, M., Chait, B. T., and MacKinnon, R. (2001) *Neuron 29*, 593−601.
5. Jiang, Y. X., Lee, A., Chen, J. Y., Cadene, M., Chait, B. T., and MacKinnon, R. (2002) *Nature 417*, 515−522.
6. Jiang, Y. X., Lee, A., Chen, J. Y., Ruta, V., Cadene, M., Chait, B. T., and MacKinnon, R. (2003) *Nature 423*, 33−41.
7. Blount, P., Sukharev, S. I., Moe, P. C., Martinac, B., and Kung, C. (1999) *Methods Enzymol. 294*, 458−482.
8. MacKinnon, R. (2000) *J. Gen. Physiol. 116*, 17.
9. Saimi, Y., Loukin, S. H., Zhou, X. L., Martinac, B., and Kung, C. (1999) *Methods Enzymol. 294*, 507−524.
10. Bass, R. B., Strop, P., Barclay, M., and Rees, D. C. (2002) *Science 298*, 1582−1587.
11. Dutzler, R., Campbell, E. B., and MacKinnon, R. (2003) *Science 300*, 108−112.
12. Miller, C. (1982) *Philos. Trans. R. Soc. London, Ser. B 299*, 401−411.
13. Miller, C., and White, M. M. (1984) *Proc. Natl. Acad. Sci. U.S.A. 81*, 2772−2775.
14. Walz, T., Hirai, T., Murata, K., Heymann, J. B., Mitsuoka, K., Fujiyoshi, Y., Smith, B. L., Agre, P., and Engel, A. (1997) *Nature 387*, 624−627.
15. Schrempf, H., Schmidt, O., Kummerlen, R., Hinnah, S., Muller, D., Betzler, M., Steinkamp, T., and Wagner, R. (1995) *EMBO J. 14*, 5170−5178.
16. Kuo, A., Gulbis, J. M., Antcliff, J. F., Rahman, T., Lowe, E. D., Zimmer, J., Cuthbertson, J., Ashcroft, F. M., Ezaki, T., and Doyle, D. A. (2003) *Science* (in press).
17. Zhou, Y. F., Morais-Cabral, J. H., Kaufman, A., and MacKinnon, R. (2001) *Nature 414*, 43−48.
18. Heginbotham, L., Abramson, T., and MacKinnon, R. (1992) *Science 258*, 1152−1155.
19. MacKinnon, R. (1995) *Neuron 14*, 889−892.
20. Heginbotham, L., Lu, Z., Abramson, T., and MacKinnon, R. (1994) *Biophys. J. 66*, 1061−1067.
21. Morais-Cabral, J. H., Zhou, Y. F., and MacKinnon, R. (2001) *Nature 414*, 37−42.
22. Nishida, M., and MacKinnon, R. (2002) *Cell 111*, 957−965.
23. Lopatin, A. N., Makhina, E. N., and Nichols, C. G. (1994) *Nature 366*−*369*.

24. Abrams, C. J., Davies, N. W., Shelton, P. A., and Stanfield, P. R. (1996) *J. Physiol. 493*, 643−649.
25. Stanfield, P. R., Davies, N. W., Shelton, P. A., Sutcliffe, M. J., Khan, S., Brammar, W. J., and Conley, E. C. (1994) *J. Physiol. 478*, 1−6.
26. Perozo, E., Santacruz-Toloza, L., Stefani, E., Bezanilla, F., and Papazian, D. M. (1994) *Biophys. J. 66*, 345−354.
27. Tytgat, J., Nakazawa, K., Gross, A., and Hess, P. (1993) *J. Biol. Chem. 268*, 23777−23779.
28. Bezanilla, F. (2000) *Physiol. Rev. 80*, 555−592.
29. Jiang, Y. X., Ruta, V., Chen, J. Y., Lee, A., and MacKinnon, R. (2003) *Nature 423*, 42−48.
30. Lu, Z., Klem, A. M., and Ramu, Y. (2001) *Nature 413*, 809−813.
31. Slatin, S. L., Qiu, X. Q., Jakes, K. S., and Finkelstein, A. (1994) *Nature 371*, 158−161.
32. Chen, G. Q., Cui, C. H., Mayer, M. L., and Gouaux, E. (1999) *Nature 402*, 817−821.
33. Mayer, M. L., Olson, R., and Gouaux, E. (2001) *J. Mol. Biol. 311*, 815−836.
34. Cheng, Q., Thiran, S., Yernool, D., Gouaux, E., and Jayaraman, V. (2002) *Biochemistry 41*, 1602−1608.
35. Armstrong, N., and Gouaux, E. (2000) *Neuron 28*, 165−181.
36. Ren, D. J., Navarro, B., Xu, H. X., Yue, L. X., Shi, Q., and Clapham, D. E. (2001) *Science 294*, 2372−2375.
37. Maduke, M., Pheasant, D. J., and Miller, C. (1999) *J. Gen. Physiol. 114*, 713−722.
38. Maduke, M., Miller, C., and Mindell, J. A. (2000) *Annu. Rev. Biophys. Biomol. Struct. 29*, 411−438.
39. Pusch, M., Ludewig, U., Rehfeldt, A., and Jentsch, T. J. (1995) *Nature 373*, 527−531.
40. Estevez, R., Schroeder, B. C., Accardi, A., Jentsch, T. J., and Pusch, M. (2003) *Neuron 38*, 47−59.
41. Jiang, Y. X., Lee, A., Chen, J. Y., Cadene, M., Chait, B. T., and MacKinnon, R. (2002) *Nature 417*, 523−526.
42. Perozo, E., Cortes, D. M., and Cuello, L. G. (1999) *Science 285*, 73−78.
43. del Camino, D., Holmgren, M., Liu, Y., and Yellen, G. (2000) *Nature 403*, 321−325.
44. Holmgren, M., Smith, P. L., and Yellen, G. (1997) *J. Gen. Physiol. 109*, 527−535.
45. Chen, T., and Miller, C. (1996) *J. Gen. Physiol. 108*, 237−250.
46. Iyer, R., Iverson, T. M., Accardi, A., and Miller, C. (2002) *Nature 419*, 715−718.
47. Foster, J. W., Moreno, M. (1999) in *Bacterial Response to pH*, John Wiley & Sons, Ltd: Chichester, England, pp 55−74.
48. Cuello, L. G., Romero, J. G., Cortes, D. M., and Perozo, E. (1998) *Biochemistry 37*, 3229−3236.
49. Irizarry, S. N., Kutluay, E., Drews, G., Hart, S. J., and Heginbotham, L. (2002) *Biochemistry 41*, 13653−13662.
50. Munro, A. W., Ritchie, G. Y., Lamb, A. J., Douglas, R. M., and Booth, I. R. (1991) *Mol. Microbiol. 5*, 607−616.
51. Meury, J., and Kepes, A. (1982) *EMBO J. 1*, 339−343.
52. Ferguson, G. P., Mclaggan, D., and Booth, I. R. (1995) *Mol. Microbiol. 17*, 1025−1033.
53. Elmore, M. J., Lamb, A. J., Ritchie, G. Y., Douglas, R. M., Munro, A., Gajewska, A., and Booth, I. R. (1990) *Mol. Microbiol. 4*, 405−412.
54. Ferguson, G. P., Totemeyer, S., MacLean, M. J., and Booth, I. R. (1998) *Arch. Microbiol. 170*, 209−218.
55. Roosild, T. P., Miller, S., Booth, I. R., and Choe, S. (2002) *Cell 109*, 781−791.
56. Miller, S., Douglas, R. M., Carter, P., and Booth, I. R. (1997) *J. Biol. Chem. 272*, 24942−24947.
57. Ness, L. S., and Booth, I. R. (1999) *J. Biol. Chem. 274*, 9524−9530.
58. Magnusson, U., Chaudhuri, B. N., Ko, J., Park, C., Jones, T. A., and Mowbray, S. L. (2002) *J. Biol. Chem. 277*, 14077−14084.
59. Booth, I. R. (1985) *Microbiol. Rev. 49*, 359−378.
60. Booth, I. R., Cash, P., and O'Byrne, C. (2002) *Antonie van Leeuwenhoek 81*, 33−42.
61. Durell, S. R., Hao, Y. L., Nakamura, T., Bakker, E. P., and Guy, H. R. (1999) *Biophys. J. 77*, 775−788.
62. Maser, P., Hosoo, Y., Goshima, S., Horie, T., Eckelman, B., Yamada, K., Yoshida, K., Bakker, E. P., Shinmyo, A., Oiki, S., Schroeder, J. I., and Uozumi, N. (2002) *Proc. Natl. Acad. Sci. U.S.A. 99*, 6428−6433.
63. Ferguson, G. P., Munro, A. W., Douglas, R. M., Mclaggan, D., and Booth, I. R. (1993) *Mol. Microbiol. 9*, 1297−1303.
64. Ferguson, G. P., Battista, J. R., Lee, A. T., and Booth, I. R. (2000) *Mol. Microbiol. 35*, 113−122.
65. Locher, K. P., Lee, A. T., and Rees, D. C. (2002) *Science 296*, 1091−1098.
66. Cowan, S. W., Schirmer, T., Rummel, G., Steiert, M., Ghosh, R., Pauptit, R. A., Jansonius, J. N., and Rosenbusch, J. P. (1992) *Nature 358*, 727−733.
67. Dutzler, R., Schirmer, T., Karplus, M., and Fischer, S. (2002) *Structure 10*, 1273−1284.
68. Sun, H., Tsunenari, T., Yau, K. W., and Nathans, J. (2002) *Proc. Natl. Acad. Sci. U.S.A. 99*, 4008−4013.
69. Goodstadt, L., and Ponting, C. R. (2001) *Hum. Mol. Genet. 10*, 2209−2214.

BI034953W